Molecular Vision 2019; 25:129-142 <http://www.molvis.org/molvis/v25/129>
Received 8 September 2018 | Accepted 15 February 2019 | Published 17 February 2019

Ocular phenotypic consequences of a single copy deletion of the *Yap1* gene (*Yap1*$^{+/-}$) in mice

Soohyun Kim,[1] Sara M. Thomasy,[1,2] Vijay Krishna Raghunathan,[3,4,5] Leandro B.C. Teixeira,[6] Ala Moshiri,[2] Paul FitzGerald,[2,7] Christopher J. Murphy[1,2]

[1]Department of Surgical and Radiological Sciences, School of Veterinary Medicine, University of California Davis, Davis, CA; [2]Department of Ophthalmology & Vision Science, School of Medicine, School of Medicine, University of California Davis, Davis, CA; [3]Department of Basic Sciences, College of Optometry, University of Houston, Houston, TX; [4]The Ocular Surface Institute, College of Optometry, University of Houston, Houston, TX; [5]Department of Biomedical Engineering, Cullen College of Engineering, University of Houston, Houston, TX; [6]Comparative Ocular Pathology Laboratory of Wisconsin, Department of Pathobiological Sciences, School of Veterinary Medicine, University of Wisconsin-Madison, Madison, WI; [7]Department of Cell Biology and Human Anatomy, School of Medicine, School of Medicine, University of California Davis, Davis, CA

Purpose: To identify the effects of a single copy deletion of *Yap1* (*Yap1*$^{+/-}$) in the mouse eye, the ocular phenotypic consequences of *Yap1*$^{+/-}$ were determined in detail.

Methods: Complete ophthalmic examinations, as well as corneal esthesiometry, the phenol red thread test, intraocular pressure, and Fourier-domain optical coherence tomography were performed on *Yap1*$^{+/-}$ and age-matched wild-type (WT) mice between eyelid opening (2 weeks after birth) and adulthood (2 months and 1 year after birth). Following euthanasia, enucleated eyes were characterized histologically.

Results: Microphthalmia with small palpebral fissures, corneal fibrosis, and reduced corneal sensation were common findings in the *Yap1*$^{+/-}$ mice. Generalized corneal fibrosis precluded clinical examination of the posterior structures. Histologically, thinning and keratinization of the corneal epithelium were observed in the *Yap1*$^{+/-}$ mice in comparison with the WT mice. Distorted collagen fiber arrangement and hypercellularity of keratocytes were observed in the stroma. Descemet's membrane was extremely thin and lacked an endothelial layer in the *Yap1*$^{+/-}$ mice. The iris was adherent to the posterior cornea along most of its surface creating a distorted contour. Most of the *Yap1*$^{+/-}$ eyes were microphakic with swollen fibers and bladder cells. The retinas of the *Yap1*$^{+/-}$ mice were normal at 2 weeks and 2 months of age, but the presence of retinal abnormalities, including retinoschisis and detachment, was markedly increased in the *Yap1*$^{+/-}$ mice at 1 year of age.

Conclusions: The results show that the heterozygous deletion of the *Yap1* gene in mice leads to complex ocular abnormalities, including microphthalmia, corneal fibrosis, anterior segment dysgenesis, and cataract.

Yes-associated protein (YAP) is a transcriptional coactivator encoded by the gene *YAP1* (Gene ID 22601; OMIM 606608) [1] which activates gene expression by associating with numerous DNA-binding transcription factors [2]. YAP is a key component of the Hippo signaling pathway which plays essential roles in development, organ growth, homeostasis, and cancer [3-5]. *Yap1* is essential for the development of multiple organs by regulating cell proliferation including the eye [3,6,7]. Homozygous deletion of the *Yap1* gene is known to be lethal to embryos around E8.5 to E9.5 with no evidence of attachment of the allantois to the chorion and failure of ventral closure and turning [8]. However, mice that have single gene deletion of *Yap* (*Yap1*$^{+/-}$) are viable [8], and a heterozygous mutation in *YAP1* has been reported to cause optic fissure closure defects associated with microphthalmia, cataract, and iris coloboma in humans [7].

Expression of YAP is intimately involved in eye development and corneal wound healing. Whole-mount in situ hybridization in mouse embryos has shown that *Yap1* is strongly expressed in the eye [7]. YAP expression has been documented within an array of ocular tissues, including the corneal epithelial and endothelial cells, lens epithelial cells, ciliary body, iris, inner nuclear layer of the retina, and the RPE, in the adult mouse eye [9]. In addition, YAP and TAZ are reported to be key molecules that participate in major signaling pathways relevant to corneal wound healing: mechanotransduction [10], wingless/integrated (Wnt) [11], and transforming growth factor beta (TGF-β) [12,13]. They have also been shown to act as mechanotransducers relaying the biophysical attributes of the extracellular matrix into the cells, a process that ultimately influences cell functions [13-16]. Therefore, it is likely that manipulation of the *Yap1* gene would affect corneal wound healing.

Correspondence to: Christopher J. Murphy, UC Davis School of Veterinary Medicine Surgical and Radiological Sciences, 1220 Tupper, 1 Shield Avenue, Davis, CA 95616; Phone: (530) 752-0926; FAX: (530) 752-7308; email:cjmurphy@ucdavis.edu

Mice with heterozygous deletion of the *Yap1* gene are viable, but the detailed phenotypic consequences to ocular structures have not been reported. To address the feasibility of using *Yap1*$^{+/-}$ mice as a corneal wound healing model, the present study was undertaken to determine how a single copy deletion of *Yap1* affects ocular phenotypes in mice with an emphasis on examining consequences on the cornea.

METHODS

Animals: Five *Yap1* heterozygous (*Yap1*$^{+/-}$) male C57BL/6J mice from the Knock Out Mouse Program (KOMP) within the Mouse Biology Program (MBP) at University of California, Davis and 20 female wild-type (WT) C57BL/6J mice from The Jackson Laboratory (Sacramento, CA) were used to generate *Yap1*$^{+/-}$ mice. Due to the poor fertility of female *Yap1*$^{+/-}$ mice, male *Yap1*$^{+/-}$ mice were used to mate with WT females. A total of 318 pups were generated from breeding of these initial 25 mice. All procedures were performed in compliance with the Association for Research in Vision and Ophthalmology (ARVO) Statement for the Use of Animals in Ophthalmic and Vision Research. The study design was approved by the Institutional Animal Care and Use Committee of the University of California, Davis.

Generation of a single gene deletion of Yap1: Yap1$^{+/-}$ male mice were obtained from the KOMP within the MBP. Mice were cryorecovered via in vitro fertilization using C57BL/6N oocyte donors and *Yap1* heterozygous sperm preserved by the KOMP. Fertilized two-cell stage embryos were then transferred surgically to two pseudopregnant CD1 recipients. Pseudopregnancy was induced by mating with sterile vasectomized male mice on day 0, and the manipulated embryos were transferred into these recipients a half day later. Derived pups were genotyped via short-range mutant PCR specific to *Yap1* mice with the following primers; CSD-Yap1-SR1: 5′-CAG GCA AGT TTG AGG CTA GTT TCT GG-3′, and Common-loxP-F: 5′-GAG ATG GCA ACG CAA TTA AT-3′. Male *Yap1*$^{+/-}$ mice C57BL/6J were used to breed to WT C57BL/6J females to generate *Yap1*$^{+/-}$. All *Yap1*$^{+/-}$ mice were tested for the retinal degeneration (Rd8) mutation, and positive Rd8 mutant animals were excluded from breeding to generate *Yap1*$^{+/-}$ without the Rd8 mutation. This was critical as the Rd8 background has several ocular background findings that may have confounded the study [17,18].

Genotyping: Pups were genotyped with PCR as follows. DNA was extracted from toe clip samples at 7 days after birth or tail clip samples approximately 3 weeks after birth using a DNA extraction kit (DNeasy® Blood & Tissue Kit; QIAGEN Sciences, MD) following the manufacturer's protocol. The extracted DNA was then confirmed for mutant allele copy number using PCR with the following oligonucleotides: YAP5′: CSD-lacF: 5′-GCT ACC ATT ACC AGT TGG TCT GGT GTC-3′ and YAP3′: CSD-YAP1-R: 5′-TCA AGG CCA TCA TAG ATC CTG GAC G-3′, following thermal cycling: 94 °C for 5 min; 10 cycles of 94 °C for 15 s, 65 °C for 30 s (decrease 1 °C for each cycle), 72 °C for 40 s; 30 cycles of 94 °C for 15 s, 55 °C for 30 s, 72 °C for 40 s; 72 °C for 5 min and hold at 4 °C. The PCR fragments were separated on the E-Gel® 2% Agarose with SYBR Safe™ (Invitrogen, Carlsbad, CA) at 48 V for 45 min using dry-gel system (iBase™; Invitrogen) and read with the ChemiDoc-It®2 810 Imager (UltraViolet Products Ltd., Cambridge, UK).

Ophthalmic examination and advanced ocular imaging: Ophthalmic examination and advanced ocular imaging were performed using 26 *Yap1*$^{+/-}$ and 16 WT mice within three different age groups (Appendix 1B): 2 weeks old (weaning period, eye opening time point; n=6, three *Yap1*$^{+/-}$ and three WT mice), 2 months old (adult; n=15, eight *Yap1*$^{+/-}$ and seven WT mice), and 1 year old (aged adult; n=21, fifteen *Yap1*$^{+/-}$ and six WT mice). For the ophthalmic examination and subsequent measurements, the mice were gently restrained without any pressure to their neck and head. Cochet-Bonnet esthesiometry (Esthesiometer 12/100 mm; LUNEAU Ophthalmologi, Prunay-le-Gillon, France) to determine corneal sensation, a phenol red thread test (PRTT; Zone-Quick, Showa Yakuhin Kako Co., LTD, Tokyo, Japan) to assess aqueous tear production, and rebound tonometry (TonoLab; Icare, Helsinki, Finland) to measure intraocular pressure (IOP) were performed. All mice then received a thorough ophthalmic examination of the anterior and posterior segment using a hand-held slit-lamp (Kowa SL15; Kowa Optimed, Torrance, CA) and indirect ophthalmoscopy (Keeler VANTAGE Plus; Keeler Inc., Broomall, PA) with a 90 D indirect lens (Volk Optical, Inc., Mentor, OH). Following this examination, the mice were sedated with an intraperitoneal (IP) injection of midazolam/hydromorphone (0.7 mg/kg/0.1 mg/kg) for advanced ocular imaging. The palpebral fissure length was measured with digital calipers accurate to 0.1 mm (Fred V. Fowler Co., Inc., Newton, MA). The eyes were photographed with a digital color camera (Canon EOS5D; flash 1/64. ios 200, F16) and slit-lamp biomicroscopy with digital capture (Hagg-Streit BQ 900 Slit Lamp; Haggstreit, Koeniz, Switzerland). Corneas were imaged with an RTVue-100 Fourier-Domain Optic Coherence Tomography (FD-OCT) system (software version 6.1; Optovue Inc., Fremont, CA; 26,000 A scan/sec, 5 µm axial resolution, 840 nm superluminescent diode) with a CAM-S [S/N 30,107] lens.

Tissue processing for histology and immunofluorescence staining: Mice were euthanized with pentobarbital (200 mg/

kg, IP), and body length was measured with a digital caliper (Fred V. Fowler Co., Inc.). After enucleation of both eyes, one eye of each mouse was fixed using the freeze substitution protocol as described by Sun et al. [19], and the opposite eye was dedicated for transmission electron microscopy as described below. Briefly, the enucleated mouse eyes were rapidly frozen by immersion in liquid propane at −80 °C for 1 min and then rapidly transferred to 97% methanol and 3% acetic acid at −80 °C. The samples were placed at −80 °C for 48 h and then gradually warmed every 4 h of incubation at −40 °C, −20 °C, and then 20 °C for 48 h. The fixed eyes were then processed using standard protocols and embedded in paraffin wax. Five-micrometer-thick parasagittal sections were obtained from paraffin blocks and stained with hematoxylin and eosin (H&E). Immunofluorochemistry was performed on the 5-µm-thick paraffin-embedded parasagittal sections. Paraffin was dissolved in xylene for 10 min twice, and the samples were rehydrated using a serial dilution of ethanol. After the slides were blocked in 0.03% H_2O_2 in methanol for 30 min, antigen retrieval was performed by immersing the sample in sodium citric buffer (pH 6.0) with 0.02% Tween-20 in a steamer 56 °C for 30 min, and then cooled to room temperature. Rabbit monoclonal anti-YAP antibody (Cell Signaling Technology, Danvers, MA) at 1:200 dilution in blocking buffer was incubated with the samples for 2 h in 37 °C. The samples were incubated with an appropriate secondary antibody (1:200 dilution, Thermo Scientific Pierce, Rockford, IL) at room temperature for 45 min in the dark. Nuclei were counterstained with 4'-6-diamidino-2-phenylindole (DAPI; Life Technologies, Carlsbad, CA). The stained sections were imaged using an Axiovert 200M epifluorescent microscope (Carl Zeiss Ag, Oberkochen, Germany) with a 20X objective. All images were taken with equal exposure times.

Transmission electron microscopy: The opposite eye of each mouse was fixed in 2.5% glutaraldehyde and 2% paraformaldehyde in 0.1 M sodium cacodylate buffer, and electron microscopy of the cornea was performed using standard protocols. Briefly, the fixed eyes were rinsed in 0.1 M sodium cacodylate buffer for 15 min twice and then placed in 2% osmium tetroxide for 1 h. The samples were then rinsed in water for 15 min twice. Then, the eyes were dehydrated in 50% ethyl alcohol (EtOH), 75% EtOH, and 95% EtOH for 30 min each and 100% EtOH for 20 min twice. The eyes were then placed in propylene oxide for 15 min twice. Next, the eyes were infiltrated in a Poly/Bed 812 mixture for 4 h and polymerized in a Poly/Bed 812 mixture at 65 °C for at least 24 h. Ultrathin sections were mounted on naked copper grids and stained with 3% uranyl acetate and 0.03% lead citrate before examination with a transmission electron microscope (TEM; Philips CM120 Biotwin Lens, F.E.I. Company, Hillsboro, OR; with Gatan MegaScan, model 794/20, digital camera (2 K × 2 K), Pleasanton, CA; Gatan BioScan, model 792, Pleasanton, CA).

Statistical analysis: Statistical analysis was performed with a commercially available statistical software program (GraphPad Prism 7.03, GraphPad Software Inc., San Diego, CA). Unpaired Student *t* tests with Welch's correction were performed to compare the corneal thickness measurements between the groups. An odds ratio (OR) was calculated to evaluate the incidence rate of female *Yap1*$^{+/-}$ pups with a Fisher's exact test. A p value of less than 0.05 was considered statistically significant. Results were expressed as mean ± standard deviation (SD).

RESULTS

A lower number of Yap1$^{+/-}$ *progeny than expected were identified:* Genotyping with PCR was performed on 318 pups of which 285 were WT mice and 33 were *Yap1*$^{+/-}$ mice. Given that the expected ratio should be 50% WT and 50% *Yap1*$^{+/-}$ mice, the number of *Yap1*$^{+/-}$ mice identified was statistically significantly less than the WT mice (Observed %=10.38, 95% confidence interval [CI]: 7.458 to 14.22; p<0.001). In addition, we observed a statistically significantly lower number of female versus male *Yap1*$^{+/-}$ progeny at eight and 25 mice, respectively (OR=0.387, 95% CI: 0.1794 to 0.902; p=0.025). Generally, the body length of the *Yap1*$^{+/-}$ mice (26.53±1.39 mm) was statistically significantly shorter than that of the age-matched WT mice (47.68±5.83 mm) at the weaning period (p=0.02), but adult mice were comparable (Table 1). Around 80% of the *Yap1*$^{+/-}$ mice had abnormal dome-shaped heads (Figure 1A), and some *Yap1*$^{+/-}$ mice were euthanized because of abnormal seizure-like activity (n=4) or corneal perforation (n=3).

Multiple ocular abnormalities were identified on ophthalmic examination: Similar ocular phenotypes were observed in *Yap1*$^{+/-}$ mice at the ages examined. Microphthalmia with a small palpebral fissure was observed in 67% of the *Yap1*$^{+/-}$ mice (Figure 1A) with 23% of the eyes of the *Yap1*$^{+/-}$ mice had no ocular structures clinically detectable with slit-lamp evaluation (Table 2). Generalized corneal fibrosis was present in 85% of the *Yap1*$^{+/-}$ eyes as assessed with slit-lamp biomicroscopy (Table 2) which often precluded clinical examination of the intraocular structures (Figure 1B). Three *Yap1*$^{+/-}$ mice were euthanized due to corneal perforation occurring between 2 and 6 months of age, and one eye of a *Yap1*$^{+/-}$ mouse at 2 months of age developed a perforated cornea with granulation tissue (Figure 1B). Using FD-OCT, a thin cornea with the iris adhered to the posterior aspect and aphakia were commonly

Table 1. Ocular biometry findings and diagnostics test results for *Yap1*$^{+/-}$ and wild-type (WT) mice.

Age	Genotype	Body length (mm)	Corneal touch threshold (Aesthesiometry; mm)	PRTT (mm)	IOP (mmHg)	Length of palpebral aperture (mm)	Corneal thickness (FD-OCT; µm)	Corneal thickness (histology; µm)
2-weeks	WT	47.68±5.83	-	3.51±1.29	9.8±1.3	2.68±0.19	67.0±13.2	75.9±4.1
	Yap1$^{+/-}$	*26.53±1.39	-	2.05±0.99	10.7±0.9	*1.71±0.61	*39.1±5.5	*34.2±7.2
2 months	WT	81.67±8.75	52.3±6.7	2.09±0.99	13.3±2.9	3.52±0.23	79.3±9.6	75.4±7.9
	Yap1$^{+/-}$	83.33±6.05	*30.8±8.3	1.54±0.46	13.5±3.9	*2.50±1.04	*57.1±29.0	*56.3±12.8
1-year	WT	95.56±2.67	48.6±6.0	2.88±0.99	11.2±1.2	4.85±0.41	87.3±4.6	83.2±1.5
	Yap1$^{+/-}$	92.83±6.43	*36.9±8.5	2.26±1.00	11.3±3.1	*3.60±1.25	*47.9±29.3	*59.5±17.0

PRTT, phenol red tread test (mm); IOP, intraocular pressure (mmHg); FD-OCT, Fourier-domain optic coherence tomography. *p<0.05 between *Yap1*$^{+/-}$ and wild-type mice of the same age as determined by Student *t* test.

observed in the *Yap1*$^{+/-}$ mice (Figure 2). The central corneal thickness (CCT) of the *Yap1*$^{+/-}$ mice was significantly thinner at all ages as measured with FD-OCT ($p<0.05$; Table 1). Only six eyes (two eyes in two 2-month-old mice and four eyes in three 1-year-old mice) of five *Yap1*$^{+/-}$ mice had corneas with adequate transparency allowing documentation of hypermature cataract and posterior synechiae (Figure 1B and Figure 2). The five *Yap1*$^{+/-}$ mice with clear corneas were related along paternal lines (Appendix 1C). The anterior segment and fundus of the WT mice were normal on clinical examination and FD-OCT.

The palpebral fissures in the *Yap1*$^{+/-}$ mice were significantly shorter than those in the WT mice at all ages ($p<0.01$; Table 1). Corneal touch threshold, as measured with Cochet-Bonnet estheiometry, was significantly lower in the *Yap1*$^{+/-}$ versus WT mice ($p<0.001$), but tear production as measured with the PRTT ($p>0.05$), and intraocular pressure ($p>0.05$) as measured with rebound tonometry did not differ statistically significantly between the *Yap1*$^{+/-}$ and the WT mice for the three age groups tested (Table 1). Moreover, the IOP of the *Yap1*$^{+/-}$ eyes which had clear corneas and normal anterior chamber depths showed no statistically significant differences compared with the *Yap1*$^{+/-}$ eyes with microphthalmia and corneal fibrosis at 2 months (13.5±2.1 mmHg in two clear corneal eyes versus 13.5±3.9 mmHg in the abnormal eyes; $p>0.999$) and 1 year of age (10.0±0.0 mmHg in three clear corneal eyes versus 11.6±3.2 mmHg in the abnormal eyes; $p=0.865$).

YAP expression was lower in Yap1$^{+/-}$ *versus WT mice:* YAP expression was detected in the corneal epithelium and endothelium and non-pigmented epithelium of the ciliary body in all groups of the *Yap1*$^{+/-}$ and WT mice and primarily localized to the cytoplasm in both groups. The expression of YAP was reduced in the *Yap1*$^{+/-}$ mice compared with WT mice (Figure 3). Interestingly, *Yap1*$^{+/-}$ mice with clear corneas had greater expression of YAP versus those with corneal fibrosis but had less expression in comparison with the WT mice (Appendix 2).

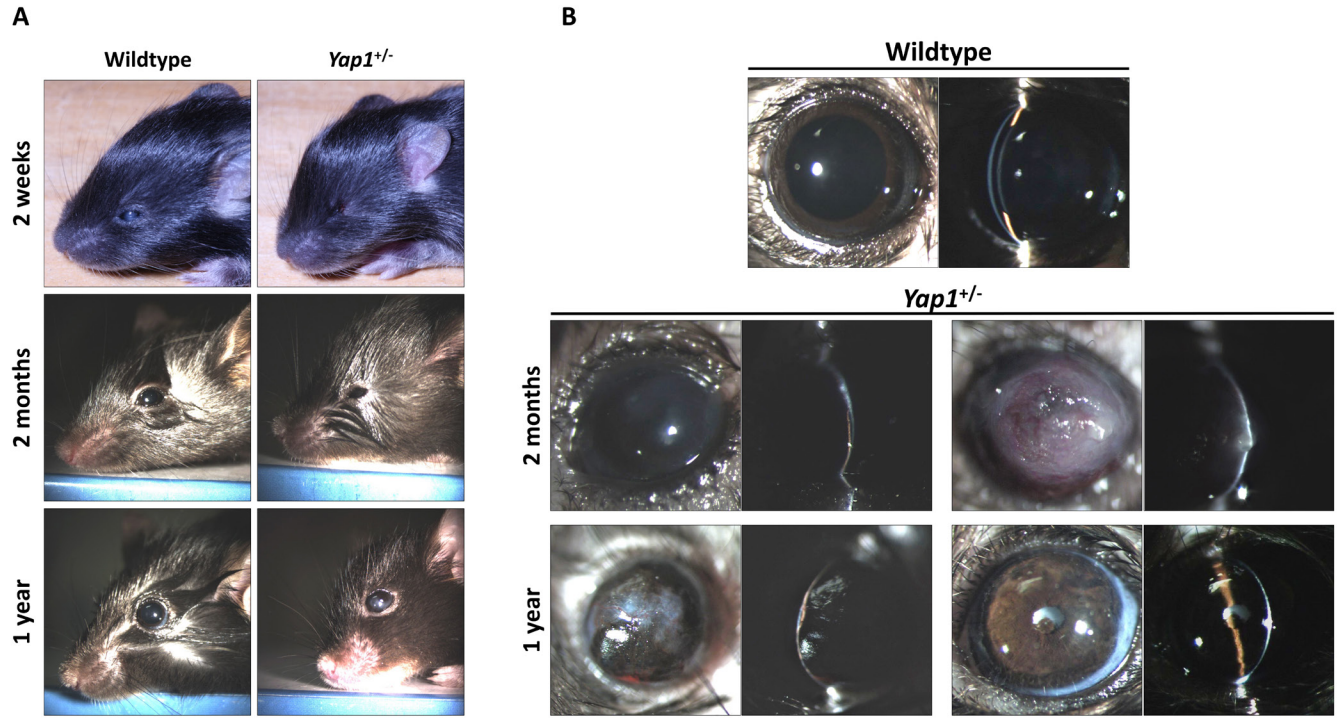

Figure 1. Microphthalmia with anterior segment dysgenesis in *Yap1*$^{+/-}$ mice. Many *Yap1*$^{+/-}$ mice were microphthalmic with anterior segment dysgenesis in comparison to age-matched WT littermates. **A**: Compared with the wild-type (WT) mouse, microphthalmia with a small palpebral fissure was identified at all ages of *Yap1*$^{+/-}$ mice on gross examination. **B**: A normal transparent cornea with an appropriate anterior chamber, iris, and lens are found on biomicroscopic examination with diffuse illumination (left) and narrow-slit beam (right) in the WT mice. Many *Yap1*$^{+/-}$ mice displayed generalized corneal fibrosis and a collapsed anterior chamber with the iris adherent to the posterior cornea (left eye; 2 months old; right eye; 1 year old). A perforated cornea and granulation tissue were observed in the right eye of a 1-year-old male *Yap1*$^{+/-}$ mouse. A hypermature cataract and posterior synechia with a deep anterior chamber were identified in the left eye of a 1-year-old male *Yap1*$^{+/-}$ mouse with a transparent cornea.

Table 2. Ocular findings for *Yap1*$^{+/-}$ mice by slit-lamp examination and histology.

		2-weeks		2 months		1-year	
		Slit-lamp	**Histology**	**Slit-lamp**	**Histology**	**Slit-lamp**	**Histology**
Microphthalmia*		2/6 (33%)	4/4 (100%)	3/16 (19%)	7/10 (70%)	7/30 (23%)	20/24 (83%)
Cornea	Thin epithelial layers	-	4/4 (100%)	-	7/10 (70%)	-	20/24 (83%)
	Stromal fibrosis with neovascularization and pigmentation	4/6 (60%)	4/4 (100%)	11/16 (69%)	8/10 (80%)	19/30 (63%)	21/24 (88%)
	Absence of Descemet's membrane and endothelium	-	4/4 (100%)	-	7/10 (70%)	-	20/24 (83%)
Anterior structure	Collapsed/shallow anterior chamber	4/6 (60%)	4/4 (100%)	11/16 (69%)	8/10 (80%)	19/30 (63%)	21/22[§] (96%)
	Adherence of iris cells inner aspect of the cornea	-	4/4 (100%)	-	8/10 (80%)	-	21/24 (88%)
	Loss of some iris substances with abnormal ICA structures	-	4/4 (100%)	-	7/10 (70%)	-	21/24 (88%)
Lens	No lens finding	-	0/4 (0%)	-	3/10 (30%)	-	12/24 (50%)
	Cataract (degenerated lens fibers, bladder cells, etc.)	-	4/4 (100%)	2/2 (100%)[#]	6/7[§] (86%)	4/4 (100%)[#]	12/12[+] (100%)
	Abnormal lens capsules (thin, ruptured, etc.)	-	4/4 (100%)	-	5/7[§] (71%)	-	12/12[+] (100%)
Retina	Retinoschisis	-	0/4 (0%)	-	2/10 (20%)	-	8/22[§] (36%)
	Retinal detachment	-	0/4 (0%)	-	1/10 (10%)	-	12/22[§] (55%)
	Inflammatory giant cells	-	0/4 (0%)	-	1/10 (10%)	-	15/24 (63%)
	Outer nuclear layer thinning	-	0/4 (0%)	-	2/10 (20%)	-	18/22[§] (82%)
	Disorganized retinal layer (including retinal laminal structure loss)	-	0/4 (0%)	-	1/10 (10%)	-	8/24 (33%)
	Rosette formation (in photoreceptor layer)	-	0/4 (0%)	-	1/10 (10%)	-	2/22[§] (9%)
	Separation of internal limiting membrane	-	0/4 (0%)	-	1/10 (10%)	-	2/22[§] (9%)

The results are presented with "the number of affected eyes/total examined eyes (percentages)." ICA=iridocorneal angle; *microphthalmia was evaluated clinically un-defined eyeball with closed or partial opened eyelid and was histologically measured the axial globe length comparing with age-matched WT, [#]cataract was diagnosed by slit lamp examination only in mice with adequate corneal transparency to enable visualization of the lens, [+]total number of eyes in which the lens was observed histologically, [§]excluded two eyes with completely disorganized and undeveloped retinas.

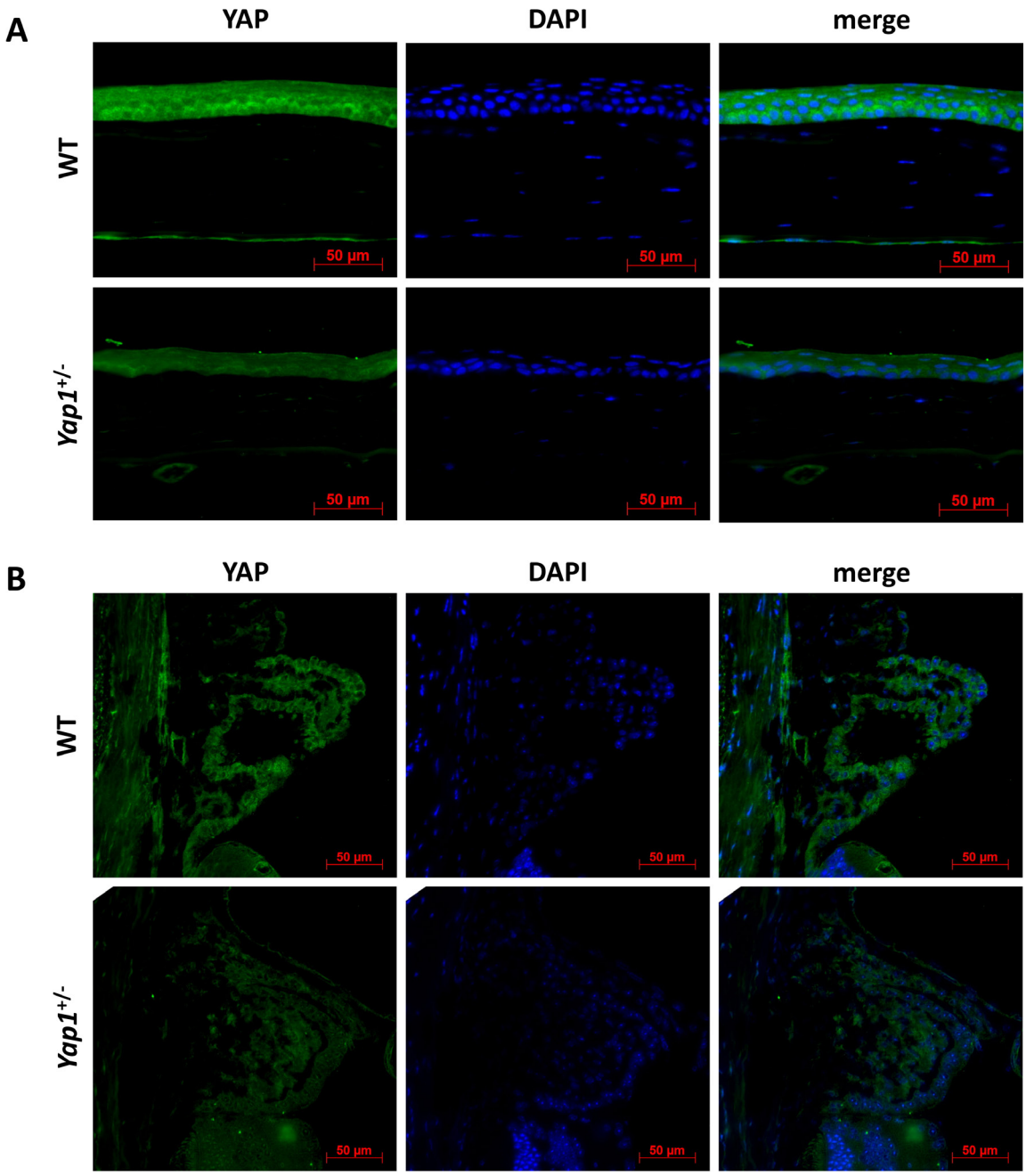

Figure 2. YAP expression in *Yap1*$^{+/-}$ and WT mice. Immunofluorescent staining showed expression of YAP in the corneal epithelium and endothelium (**A**) and non-pigmented epithelium of the ciliary body (**B**) in wild-type (WT) and *Yap1*$^{+/-}$ mice. Decreased expression of YAP was identified in *Yap1*$^{+/-}$ versus WT mice.

Histology and TEM confirmed severe corneal pathology in the Yap1$^{+/-}$ *mice:* Histologically, partial or complete collapse of the anterior chamber was observed with broad anterior synechiae in 87% of the *Yap1*$^{+/-}$ eyes (Figure 4B and Appendix 3). Iris hypoplasia with abnormal iridocorneal angle morphology was observed in 89% of the *Yap1*$^{+/-}$ eyes (Table 2). The number of corneal epithelial cell layers in the *Yap1*$^{+/-}$ mice was decreased in comparison with the WT mice (Figure 5 and Appendix 3) with loss of polygonal wing cells and superficial cells. In the corneal stroma, distorted stromal fibers, hypercellularity of corneal stromal, and rare focal edema with stromal neovascularization were observed in the

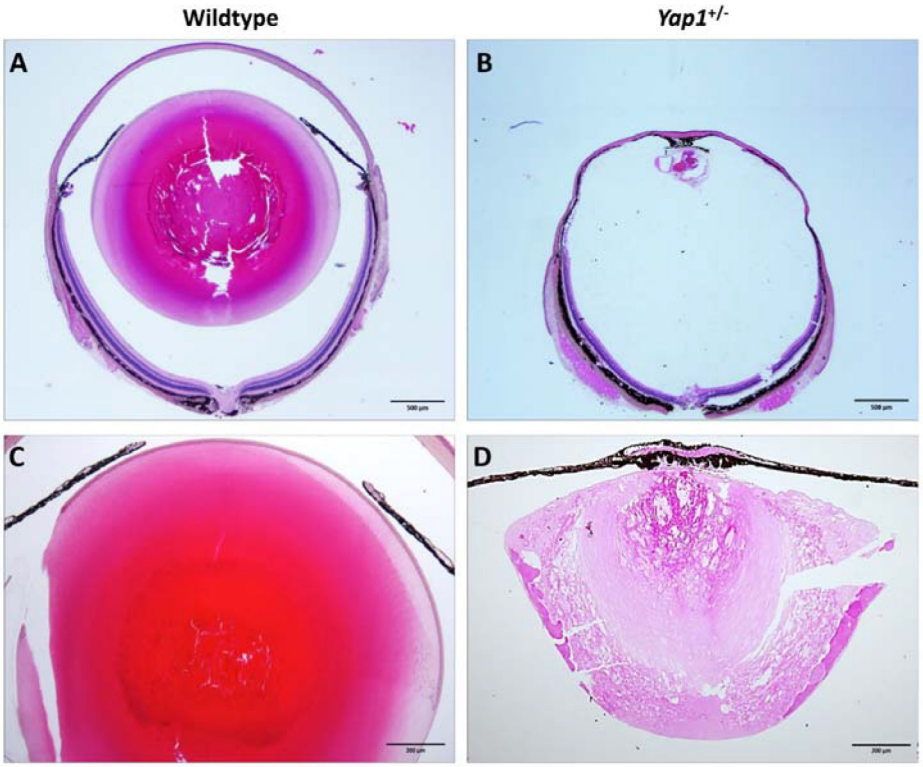

Figure 3. Anterior segment images using optic coherence tomography (OCT) in *Yap1*$^{+/-}$ and WT mice. **A**: Fourier-domain optical coherence tomography demonstrates the normal anterior segment of male wild-type (WT) mice at the indicated age: 2 weeks old, 2 months old, and 1 year old. **B**: The *Yap1*$^{+/-}$ mice demonstrate corneal pathology and anterior segment anomalies at all ages. A thin cornea with adherent iris (arrowhead), a collapsed anterior chamber, and aphakia in age-matched male *Yap1*$^{+/-}$ mice at 2 weeks old, 2 months old, and 1 year old. A small lens and a deep anterior chamber were identified in the left eye of a 1-year-old male *Yap1*$^{+/-}$ mouse. A, anterior chamber; C, cornea; I, iris; L, lens.

Yap1$^{+/-}$ mice (Figure 5B). Descemet's membrane was absent in 86% of the *Yap1*$^{+/-}$ mice eyes (Table 2).

Corneal abnormalities observed with TEM were consistent with those observed with bright-field microscopy in all ages of *Yap1*$^{+/-}$ mice with multiple ultrastructural lesions identified. In the WT mice, the corneal epithelium comprised seven to nine layers of keratinocytes with clearly identifiable differentiation among the basal, wing cell, and superficial

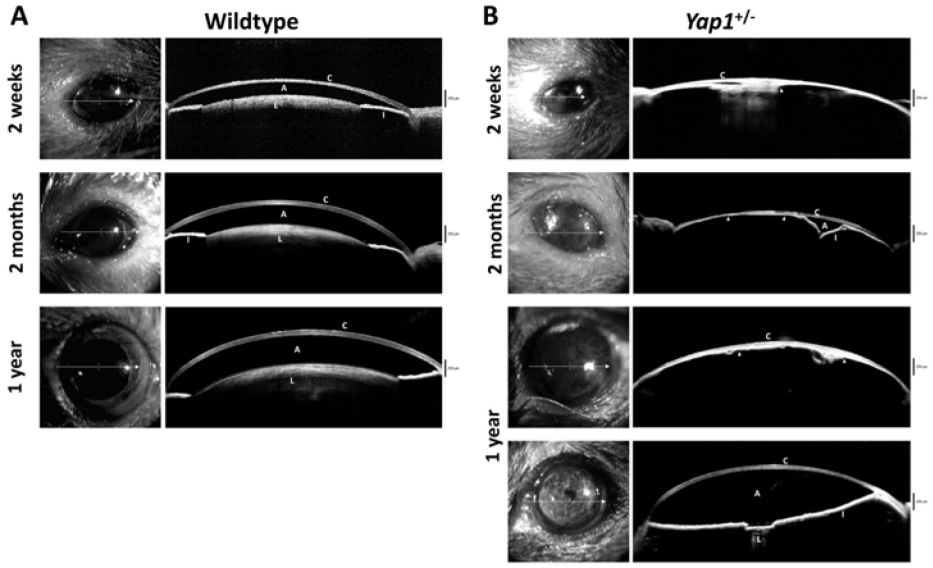

Figure 4. Histopathology of whole globes with low magnification in *Yap1*$^{+/-}$ and WT mice. Histopathology demonstrating globe size from a WT mouse with normal eyes (**A**) versus *Yap1*$^{+/-}$ mice with microphthalmia and anterior segment dysgenesis (**B**). Eyes from the *Yap1*$^{+/-}$ mice also demonstrated microphakia with cataractous changes characterized by marked degeneration and liquefaction of lens fibers, formation of Morgagnian globules, as well as bladder cells (**D**) versus age-matched WT mice with an appropriate lens size and morphology (**C**). (**A** and **B**) 2X, 1 year old; (**C** and **D**) 20X, 2 months old.

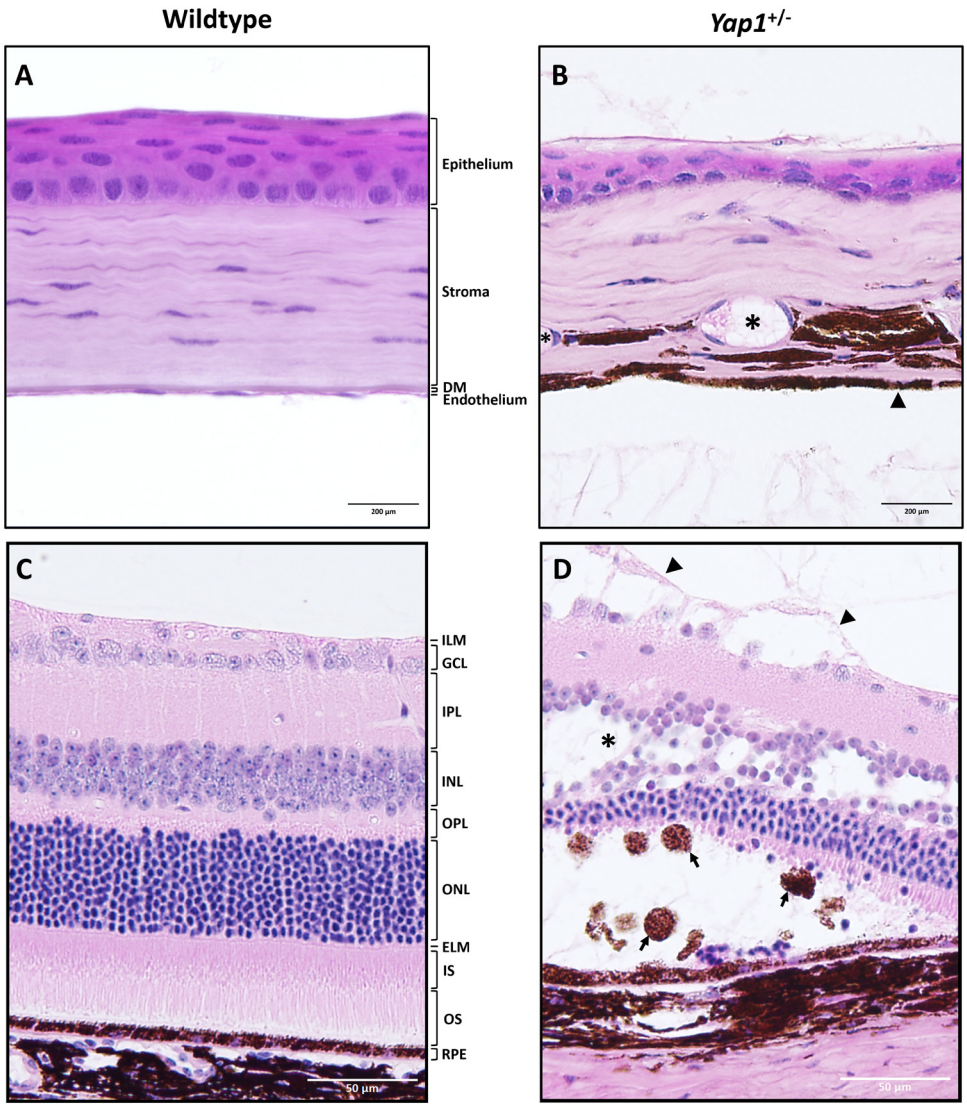

Figure 5. Histopathology of cornea and retina in the *Yap1*$^{+/-}$ and WT mice with high magnifications. Normal corneal (**A**) and retinal (**C**) morphology was observed in 1-year-old wild-type (WT) mice. In the 1-year-old *Yap1*$^{+/-}$ mice, the cornea (**B**) was diffusely thinner than in the WT mice, presenting epithelial attenuation with loss of superficial squamous cells, and hypercellular and compacted stroma with distorted lamellar arrangement and stromal neovascularization (*) and melanin pigmentation. Descemet's membrane was absent or severely thinned, and normal corneal endothelial cells were absent. In many locations, there was fusion of the iris tissue to the exposed posterior cornea stroma, and melanotic cells lined the posterior cornea in many regions where frank iris fusion was not observed (arrowheads). In 1-year-old *Yap1*$^{+/-}$ mice, retinal detachment was commonly observed and accompanied by subretinal accumulation of macrophages (arrows) and loss of photoreceptors (**D**). Retinoschisis (*) of the inner nuclear layer and separation of the internal limiting membrane from the nerve fiber layer (arrowheads) were observed. (**A** and **B**) 40X, hematoxylin and eosin (H&E); DM, Descemet's membrane. (**C** and **D**) 20X, H&E; ILM, internal limiting membrane; GCL, ganglion cell layer; IPL, inner plexiform layer; INL, inner nuclear layer; OPL, outer plexiform layer; ONL, outer nuclear layer; ELM, external limiting membrane; IS, inner segment; OS, outer segment; RPE, retinal pigment epithelium.

squamous cell layers (Figure 6A). In contrast, the *Yap1*$^{+/-}$ mice demonstrated marked thinning of the superficial squamous cell layer and a lack of microvilli on the apical surface of the most superficial keratinocytes (Figure 6B). The corneal stroma on the *Yap1*$^{+/-}$ mice showed increased cellularity due to the presence of fusiform cells between the stromal lamellae with an abundant vacuolar cytoplasm and oval nuclei, consistent with reactive keratocytes (Figure 6B); spindle-shaped keratocytes were localized between the stromal lamellae in the WT mice. The *Yap1*$^{+/-}$ mice also had a thin Descemet's membrane compared to the age-matched WT mice and lacked a recognizable endothelial cell layer, which was replaced by a layer of melanin-laden cuboidal cells (Figure 6).

Lens abnormalities were observed in Yap1$^{+/-}$ *mice of all ages:* Hypermature cataract and posterior synechiae were documented in the five *Yap1*$^{+/-}$ mice that had transparent corneas with a slit-lamp examination and imaging (Figure 1B and Figure 3); the age-matched WT mice showed no lens abnormalities. Clinical evaluation of the lens could not be performed in the remaining 28 *Yap1*$^{+/-}$ mice due to microphthalmia, corneal fibrosis, and anterior synechiae.

In cases where the lens could be identified clinically, histopathological features of included microphakia with hypermature cataract (Figure 4D). The cataractous changes were represented by marked degeneration and liquefaction

of the lens fibers, formation of morgagnian globules, bladder cells, and posterior migration of the lens epithelium in 60% of total *Yap1*$^{+/-}$ eyes or 96% of the *Yap1*$^{+/-}$ eyes where a lens was present (Table 2). In 40% of the *Yap1*$^{+/-}$ eyes, a lens could not be found on histologic evaluation, and the eyes were considered aphakic (Table 2). Additional lens findings included abnormal lens capsules (Figure 4D) and frank posterior lens capsule rupture with extruded degenerate lens fibers (Table 2).

Age-related retinal degeneration and retinoschisis were identified in the 1-year-old Yap1$^{+/-}$ *mice:* The fundus could not be clinically evaluated in any *Yap1*$^{+/-}$ mice due to opacification of the cornea or cataracts; the fundus of all WT mice was assessed as normal. Histologically, retinal morphology was typically normal in WT and *Yap1*$^{+/-}$ mice at 2 weeks and 2 months of age (Appendix 4). Persistent hyaloid artery (HA) and *tunica vasculosa lentis* (TVL) were commonly observed at 2 weeks after birth in the WT and *Yap1*$^{+/-}$ mice as normal developmental findings. Seven eyes of 2-month-old *Yap1*$^{+/-}$ mice had normal retinal morphology while two eyes had retinoschisis (n=2) and focally extensive areas of retinal detachment (n=1; Table 2). In the *Yap1*$^{+/-}$ mice, the incidence of retinal abnormalities, including retinal detachment and retinoschisis, was greater in the 1-year-old age group than in the 2-week-old and 2-month-old age groups in the *Yap1*$^{+/-}$ mice (Table 2). In the 1-year-old *Yap1*$^{+/-}$ mice, retinal detachment with loss of the RPE and subretinal accumulation of macrophages were common findings (Table 2 and Figure 5D); retinal thinning with loss of outer nuclear, photoreceptor, and RPE layers accompanied retinal detachment (Figure 5D). Retinoschisis was observed in 36% of the 1-year-old *Yap1*$^{+/-}$ mice, and it was characterized by focally extensive vacuolization of the inner nuclear layer and/or separation of the internal limiting membrane from the nerve fiber layer (Figure 5D). Rosette formation in the photoreceptor layer was also identified in two 1-year-old *Yap1*$^{+/-}$ mice.

DISCUSSION

The present study investigated the ocular phenotypic consequences of a single copy deletion of the *Yap1* gene. In addition to profound anterior segment abnormalities, the data suggest that haploinsufficiency of *Yap1* promotes embryonic death and in survivors, developmental consequences, as indicated by the shorter body length in the *Yap1*$^{+/-}$ versus WT mice,

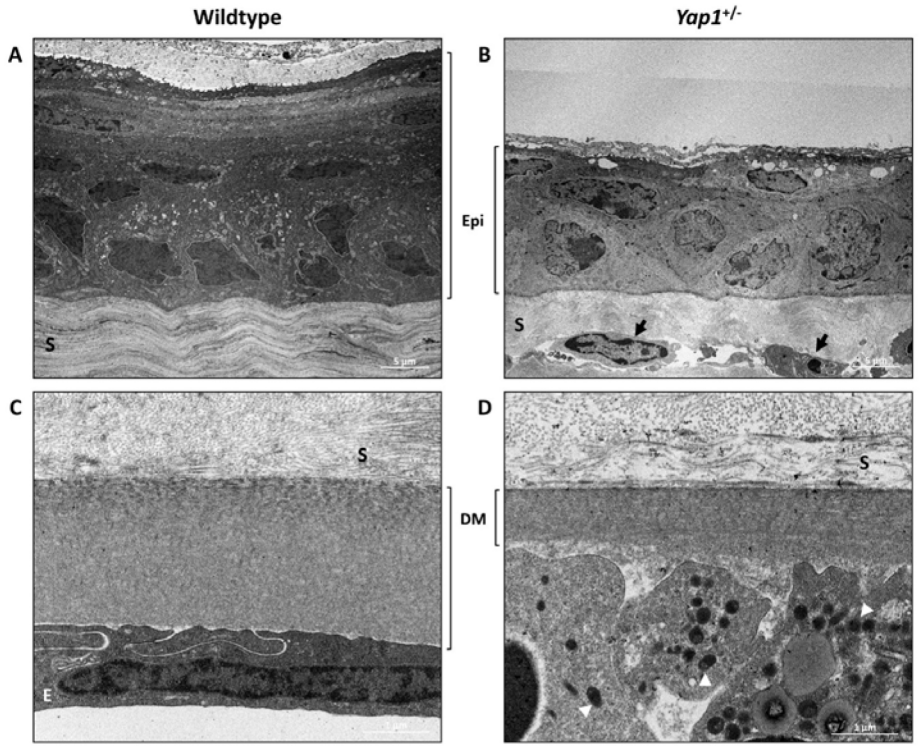

Figure 6. Corneal findings using transmission electron microscopy of 2-month-old wild-type (WT; **A** and **C**) and *Yap1*$^{+/-}$ mice (**B** and **D**). **A**: The WT mice had a normal five- to eight-layer corneal epithelium, including discernable basal columnar cells with oval nuclei, intermediate polygonal cells, and stratified squamous cells. **B**: The corneal epithelium in the *Yap1*$^{+/-}$ mice was thinner with two to four layers of cells, including a normal basal cell layer and a poorly differentiated superficial squamous layer. The corneal stroma of the *Yap1*$^{+/-}$ mice was hypercellular with cells characterized by abundant cytoplasm, numerous variable-sized vacuoles, and oval nuclei, interpreted as reactive keratocytes (black arrows). **C**: A single layer of flattened endothelial cells with well-structured gap junctions was identified resting on the normal Descemet's membrane in the WT mice. **D**: The *Yap1*$^{+/-}$ mice lacked a normal endothelium that was replaced by cuboidal melanocytes containing numerous pigment granules (melanin; white arrowheads). These cells were observed overlying an absent or markedly thinned Descemet's membrane. Epi, epithelium; S, stroma; DM, Descemet's membrane; E, endothelium.

ocular and adnexal abnormalities, and the development of a dome-shaped head in some animals. *Yap1* is required to promote early chondrocyte proliferation and its subsequent maintenance [20]. These critical functions likely contributed to the smaller body size observed in the *Yap1*$^{+/-}$ mice and may have contributed to the development of a dome-shaped head. In the present study, male *Yap1*$^{+/-}$ mice were used to mate with the WT females to generate additional *Yap1*$^{+/-}$ mice because female *Yap1*$^{+/-}$ mice are unable to be fertilized due to a lack of ovarian follicular growth [21,22]. Only 10% of the pups generated in this study were genotyped as *Yap1*$^{+/-}$ which is consistent with previous studies reporting between 12.5% and 16.7% [23]. Given the important myriad roles that YAP and Hippo signaling [8,23] play throughout development, it is unsurprising that knockout of even one copy of *Yap1* often results in embryonic death. Moreover, the phenotypic consequences of single gene deletion of *Yap1* was widely variable. A range of ocular phenotypic consequences was observed in this study. Although all animals had ocular abnormalities, the extent of the ocular involvement varied. This is best exemplified by the corneal findings that ranged from normal to markedly abnormal. This variability is likely the consequence of the interplay between the "noise" in gene expression and the complex downstream effects on regulatory networks [24,25]. Variability in phenotypic consequences for the deletion of *Yap65* has been reported in mice [8] as well as functional mutation of *YAP1* in human clinical studies [7]. Interestingly, in this study, the *Yap1*$^{+/-}$ mice possessing a clear cornea (but cataract) were all related along paternal lines, and greater expression of YAP was observed in these animals in the cornea and ciliary body than in the *Yap1*$^{+/-}$ mice with more severe corneal involvement.

The eyes of the *Yap1*$^{+/-}$ mice were often microphthalmic with a narrowed palpebral fissure consistent with previous studies in the *yap1* knockdown of *Xenopus* tadpoles [26] and the conditional knockout of *Yap* in mouse embryos [27]. YAP is a key regulator of organ size and tissue homeostasis. Hippo signaling controls organ size by phosphorylating and inhibiting the transcriptional coactivator YAP [2]. In the mouse liver, *Yap1* induction increases the organ size and causes aberrant tissue expansion [3]. Our finding of microphthalmia in the *Yap1*$^{+/-}$ eyes is consistent with these studies in other organs and suggests that YAP expression is necessary for normal eye development.

Anterior segment dysgenesis (ASD) consisting of corneal fibrosis, lack of proper formation of the anterior chamber, iris hypoplasia, and cataract were commonly observed in the *Yap1*$^{+/-}$ mice at all examined ages. In particular, the *Yap1*$^{+/-}$ mice exhibited marked cataractous changes that may be due to a close regulatory relationship between Hippo-YAP signaling or the Notch/Wnt signaling pathway. *Yap* is shown to activate target genes in Wnt signaling [28]. Hippo-YAP signaling is critical to lens development by modulating Notch signaling and subsequent lens epithelial cell migration [29,30].

Numerous ocular developmental studies in mice support that improper lens development can result in abnormal anterior segment formation [31,32]. Signals from the lens epithelium are required for proper differentiation of the cells that form the anterior structures of the eye, including the corneal endothelium [33,34] and the ciliary epithelium [35]. Neural crest-derived mesenchymal cells also contribute to the proper development of the iris, ciliary process, corneal stroma, and endothelium [31,36]. In aggregate, it is clear the lens is important for the mesenchymal-to-epithelial transformation that accompanies the formation of the corneal endothelium. Thus, the markedly thin or absent Descemet's membrane without an endothelium observed in most of the *Yap1*$^{+/-}$ mice may be a result of abnormal lens development.

YAP and TAZ are known to be present in the normal human trabecular meshwork (HTM) [14], and the expression of YAP is dramatically influenced by substratum compliance in primary HTM cells [16]. Moreover, a stiffer HTM associated with primary open angle glaucoma results in nuclear localization of YAP and TAZ that subsequently increases gene expression [16]. In this study, the *Yap1*$^{+/-}$ mice had an improperly formed iridocorneal angle and abnormal trabecular meshwork structures but also a poorly developed ciliary body and an absent anterior chamber suggesting that aqueous humor outflow and production are likely abnormal. Thus, these marked anterior segment changes prevented further study of the role that YAP may play in the aqueous outflow in *Yap1*$^{+/-}$ mice. When considering that the severity of clinically detected ASD does not correlate with IOP elevation in other mouse models as well as human patients [37], it is not surprising that the *Yap1*$^{+/-}$ mice demonstrated no alterations in IOP at any examined age in the present study.

YAP is reported to be essential for normal retinal development [27] and is specifically expressed in Müller cells and the RPE [9]. In the present study, the retinal architecture in the *Yap1*$^{+/-}$ mice was similar to that of their normal WT littermates at 2 weeks and 2 months of age. However, numerous retinal abnormalities were observed in the aged *Yap1*$^{+/-}$ mice, including loss of the RPE and outer nuclear and photoreceptor layers, retinal detachment, or retinoschisis. YAP signaling has various functions in the retina that are age-dependent [38]. YAP is a key regulator of RPE genesis [39], as well as cell proliferation and dedifferentiation in RPE cells [40]. Decreasing YAP expression has been reported to reduce

proliferation and increase differentiation in the postnatal mouse retina [9]. Taken together, these studies demonstrate that *Yap1* has multiple roles in retinal development and health that are consistent with the age-dependent retinal changes identified in the present study.

Retinoschisis is caused by a mutation in the retinoschisin (*RS1*) gene, known to express a cell adhesion protein that binds tightly to the surface of photoreceptors and bipolar cells to maintain the cellular organization in the retina [41]. Experimental mouse models such as the *RS1* knockout [42] and *RS1* knock-in [43] have been developed to study the clinical effects of retinoschisis. However, to the authors' knowledge a relation between retinoschisis and *Yap1* has not been reported. The present study is the first to report that retinoschisis occurs as a consequence of a single copy deletion in *Yap1*. Further studies are needed to explore the potential link(s) between the *RS1* gene and the YAP/TAZ signaling pathway.

This study focused on the phenotypic characterization of *Yap1*$^{+/-}$ eyes because our motivation was to study the role of YAP in corneal wound healing. YAP is important in corneal epithelial cell proliferation and the formation of tight junctions [15]. Moreover, because YAP is related to stem cell expression [44], alteration of YAP could cause disruption of cornmeal epithelial limbal stem cell function. Unfortunately, the marked corneal changes in the *Yap1*$^{+/-}$ mice prevented study of corneal epithelial and stromal wound healing. We note that three mice were euthanized due to the corneal perforation between 2 and 6 months of age. In contrast, no corneal abnormalities were found in any WT mice at any age. The loss of corneal integrity could be related to disruption of YAP signaling impairing the maintenance of corneal homeostasis and negatively impacting corneal wound healing. Therefore, a conditional knockout mouse would be necessary to study the role of YAP in corneal epithelial and stromal wound healing, and a recent study using such mice demonstrated that YAP signaling is crucial for corneal epithelial regeneration and wound healing [45].

In conclusion, the *Yap1*$^{+/-}$ mice demonstrated microphthalmia, hypoplastic, dysplastic, and fibrotic corneas with anterior segment dysgenesis, cataract, and retinal changes. Due to the complete loss of corneal transparency accompanied by corneal fibrosis, corneal wound healing could not be investigated using the *Yap1*$^{+/-}$ mouse suggesting that conditional knockouts are necessary. In aggregate, these results support that YAP signaling is critical for the proper formation and maintenance of the normal ocular structures in the eye.

APPENDIX 1.

Tables show (A) total number of mice with genotypes and genders generated from the initial pairs and (B) number of mice used for the examination and imaging in this study. One eye of each mouse was submitted for histology and the opposite eye was dedicated for transmission electron microscopy. *Both eyes were fixed for the H&E staining when the eyes were severe microphthalmia. (C) Pedigree structure shows paternal relationships of the 5 *Yap1*$^{+/-}$ mice with clinically normal transparent corneas. The mouse #1643 is one of *Yap1*$^{+/-}$ mice among 5 from the KOMP to produce 5 of the 318 pups included in this study. No clinical exam was performed for mice #1643 and #25. To access the data, click or select the words "Appendix 1."

APPENDIX 2.

YAP expression of a *Yap1*$^{+/-}$ mouse with a transparent cornea is greater than other *Yap1*$^{+/-}$ mice but still less than WT mice. To access the data, click or select the words "Appendix 2."

APPENDIX 3.

Microphthalmia and microphakia with cataract are common findings in all three age groups examined of *Yap1*$^{+/-}$ mice (B, G, L) in comparison to age-matched WT mice (A, F, K) under low magnification (x2). In comparison to the normal cornea (C, H, M), *Yap1*$^{+/-}$ showed collapse of the anterior chamber with broad anterior synechiae (D, E, J, N, O), stromal edema (D, I) and neovascularization (I, N) in higher magnification (x20). To access the data, click or select the words "Appendix 3."

APPENDIX 4.

Normal retinal morphology was observed in young (2 weeks and 2 months old) WT (A, B and E, F, respectively) and *Yap1*$^{+/-}$ (C, D and G, H, respectively) mice. For the *Yap1*$^{+/-}$ and WT mice examined 2 weeks after birth, a small vessel extending from the optic nerve head into the vitreous consistent with a hyaloid artery (HA) was observed. At the same time, there were small and regularly distributed vessels free floating in the vitreous chamber, suggesting the presence of a tunica vasculosa lentis (TVL). The TVL and HA are appropriate for this developmental stage. In comparison with the normal retina of 1 year old WT mice (I, J), retinal detachment accompanied with subretinal accumulation of macrophages, hypertrophy of the retinal pigment epithelial cells and light proteinaceous exudate was also observed in a mouse in one year old *Yap1*$^{+/-}$ mice with retinoschisis (K, L). Thinned retinas due to loss of outer nuclear and photoreceptor

layers were also common findings at this age in *Yap1*$^{+/-}$ mice. To access the data, click or select the words "Appendix 4."

ACKNOWLEDGMENTS

The authors thank Paul Russell for his support and Monica Motta, Ariana Marangakis, Carina Pasqualino, Madison Mukai and Daniel Madrigal for excellent technical assistance; Bradley Shibata for assistance in slide preparation and TEM imaging. This study was funded by grants from the National Institute of Health R01EY016134, R01EY019970, K08EY027463 and P30EY12576.

REFERENCES

1. Yagi R, Chen LF, Shigesada K, Murakami Y, Ito Y. A WW domain-containing Yes-associated protein (YAP) is a novel transcriptional co-activator. EMBO J 1999; 18:2551-62. [PMID: 10228168].
2. Zhao B, Tumaneng K, Guan KL. The Hippo pathway in organ size control, tissue regeneration and stem cell self-renewal. Nat Cell Biol 2011; 13:877-83. [PMID: 21808241].
3. Camargo FD, Gokhale S, Johnnidis JB, Fu D, Bell GW, Jaenisch R, Brummelkamp TR. YAP1 increases organ size and expands undifferentiated progenitor cells. Curr Biol 2007; 17:2054-60. [PMID: 17980593].
4. Dong J, Feldmann G, Huang J, Wu S, Zhang N, Comerford SA, Gayyed MF, Anders RA, Maitra A, Pan D. Elucidation of a universal size-control mechanism in drosophila and mammals. Cell 2007; 130:1120-33. [PMID: 17889654].
5. Pan D. The Hippo signaling pathway in development and cancer. Dev Cell 2010; 19:491-505. [PMID: 20951342].
6. Han D, Byun SH, Park S, Kim J, Kim I, Ha S, Kwon M, Yoon K. YAP/TAZ enhance mammalian embryonic neural stem cell characteristics in a Tead-dependent manner. Biochem Biophys Res Commun 2015; 458:110-6. [PMID: 25634692].
7. Williamson KA, Rainger J, Floyd JA, Ansari M, Meynert A, Aldridge KV, Rainger JK, Anderson CA, Moore AT, Hurlens ME, Clarke A, van Heyningen V, Verlose A, Taylor MS, Wilkie AO. UK10K Consortium, Fitzpatrick DR. Heterozygous loss-of-function mutations in YAP1 cause both isolated and syndromic optic fissure closure defects. Am J Hum Genet 2014; 94:295-302. [PMID: 24462371].
8. Morin-Kensicki EM, Boone BN, Howell M, Stonebraker JR, Teed J, Alb JG, Magnuson TR, O'Neal W, Milgram SL. Defects in yolk sac vasculogenesis, chorioallantoic fusion, and embryonic axis elongation in mice with targeted disruption of Yap65. Mol Cell Biol 2006; 26:77-87. [PMID: 16354681].
9. Hamon A, Masson C, Bitard J, Gieser L, Roger JE, Perron M. Retinal degeneration triggers the activation of YAP/TEAD in reactive Muller cells. Invest Ophthalmol Vis Sci 2017; 58:1941-53. [PMID: 28384715].
10. McMurray RJ, Dalby MJ, Tsimbouri PM. Using biomaterials to study stem cell mechanotransduction, growth and differentiation. J Tissue Eng Regen Med 2015; 9:528-39. [PMID: 25370612].
11. Lyu J, Joo CK. Expression of Wnt and MMP in epithelial cells during corneal wound healing. Cornea 2006; 25:S24-8. [PMID: 17001188].
12. Morgan JT, Murphy CJ, Russel P. What do mechanotransduction, Hippo, Wnt, and TGFβ have in common? YAP and TAZ as key orchestrating molecules in ocular health and disease. Exp Eye Res 2013; 115:1-12. [PMID: 23792172].
13. Attisano L, Wrana JL. Signal integration in TGF-β, WNT, and Hippo pathways. F1000Prime Rep 2013; 5:17-[PMID: 23755364].
14. Raghunathan VK, Morgan JT, Dreier B, Reilly CM, Thomasy SM, Wood JA, Tuyen BC, Hughbanks M, Murphy CJ, Russell P. Role of substratum stiffness in modulating genes associated with exracellular matrix and mechanotransducers YAP and TAZ. Invest Ophthalmol Vis Sci 2013; 54:378-86. [PMID: 23258147].
15. Raghunathan VK, Dreier B, Morgan JT, Tuyen BC, Rose BW, Reilly CM, Russell P, Murphy CJ. Involvement of YAP, TAZ and HSP90 in contact guidance and intercellular junction formation in corneal epithelial cells. PLoS One 2014; 9:e109811-[PMID: 25290150].
16. Thomasy SM, Morgan JT, Wood JA, Murphy CJ, Russell P. Substratum stiffness and latrunculin B modulate the gene expression of the mechanotransducers YAP and TAZ in human trabecular meshwork cells. Exp Eye Res 2013; 113:66-73. [PMID: 23727052].
17. Moor BA, Roux MJ, Sebbag L, Cooper A, Edwards SG, Leonard BC, Imai DM, Griffey S, Bower L, Clary D, Lloyd KCK, Herault Y, Thomasy SM, Murphy CJ, Moshiri A. A population study of common ocular abnormalities in C57BL/6N rd8 Mice. Invest Ophthalmol Vis Sci 2018; 59:2252-61. [PMID: 29847629].
18. Mattapallil MJ, Wawrousek EF, Chan C, Zhao H, Roychoudbury J, Ferguson TA, Caspi RR. The Rd8 mutation of the Crb1 gene is present in vendor lines of C57BL/6N mice and embryonic stem cells, and confounds ocular induced mutant phenotypes. Invest Ophthalmol Vis Sci 2012; 53:2921-7. [PMID: 22447858].
19. Sun N, Shibata B, Hess JF, FitzGerald PG. An alternative means of retaining ocular structure and improving immunoreactivity for light microscopy studies. Mol Vis 2015; 21:428-42. [PMID: 25991907].
20. Deng Y, Wu A, Li P, Li G, Qin L, Song H, Mak KK. Yap1 regulates multiple steps of chondrocyte differentiation during skeletal development and bone repair. Cell Reports 2016; 14:2224-37. [PMID: 26923596].
21. Cheng Y, Feng Y, Jansson L, Sato Y, Deguchi M, Kawamura K, Hsueh AJ. Actin polymerization-enhancing drugs promote ovarian follicle growth mediated by the Hippo signaling effector YAP. FASEB J 2015; 29:2423-30. [PMID: 25690654].

22. Xiang C, Li J, Hu L, Huang J, Luo T, Zhong Z, Zheng Y, Zheng L. Hippo signaling pathway reveals a spatio-temporal correlation with the size of primordial follicle pool in mice. Cell Physiol Biochem 2015; 35:957-68. [PMID: 25659841].

23. Wang J, Xiao Y, Hsu CW, Martinez-Traverso IM, Zhang M, Bai Y, Ishii M, Maxson RE, Olson EN, Dickinson ME, Wythe JD, Martin JF. Yap and Taz play a crucial role in neural crest-derived craniofacial development. Development 2016; 143:504-15. [PMID: 26718006].

24. Raser JM, O'Shea EK. Nosie in gene expression: origins, consequences, and control. Science 2005; 309:2010-3. [PMID: 16179466].

25. Chalancon G, Ravarani CN, Balaji S, Martinez-Arias A, Aravind L, Jothi R, Babu MM. Interplay between gene expression noise and regulatory network architecture. Trends Genet 2012; 28:221-32. [PMID: 22365642].

26. Cabochette P, Vega-Lopez G, Bitard J, Parain K, Chemouny R, Masson C, Borday C, Hedderich M, Henningfeld KA, Locker M, Bronchain O, Perron M. YAP controls retinal stem cell DNA replication timing and genomic stability. eLife 2015; 4:e08488-[PMID: 26393999].

27. Kim JY, Park R, Lee JH, Shin J, Nickas J, Kim S, Cho SH. Yap is essential for retinal progenitor cell cycle progression and RPE cell fate acquisition in the developing mouse eye. Dev Biol 2016; 419:336-47. [PMID: 27616714].

28. Heallen T, Zhang M, Wang J, Bonilla-claudio M, Klysik E, Johnson RL, Martin JF. Hippo pathway inhibits Wnt signaling to restrain cardiomyocyte proliferation and heart size. Science 2011; 332:458-61. [PMID: 21512031].

29. Song JY, Park R, Kim JY, Hughes L, Lu L, Kim S, Johnson RL, Cho SH. Dual function of Yap in the regulation of lens progenitor cells and cellular polarity. Dev Biol 2014; 386:281-90. [PMID: 24384391].

30. McAvoy JW, Dawes LJ, Sugiyama Y, Lovicu FJ. Intrinsic and extrinsic regulatory mechanisms are required to form and maintain a lens of the correct size and shape. Exp Eye Res 2017; 156:34-40. [PMID: 27109030].

31. Cavalheiro GR, Matos-Rodrigues GE, Gomes AL, Rodrigues PM, Martins RA. c-Myc regulates cell proliferation during lens development. PLoS One 2014; 9:e87182-[PMID: 24503550].

32. Medina-Martinez O, Brownell I, Amaya-Manzanares F, Hu Q, Behringer RR, Jamrich M. Severe defects in proliferation and differentiation of lens cells in Foxe3 null mice. Mol Cell Biol 2005; 25:8854-63. [PMID: 16199865].

33. Lwigale PY, Bronner-Fraser M. Semaphorin3A/neuropilin-1 signaling acts as a molecular switch regulating neural crest migration during cornea development. Dev Biol 2009; 336:257-65. [PMID: 19833121].

34. Beebe DC, Coats JM. The lens organizes the anterior segment: specification of neural crest cell differentiation in the avian eye. Dev Biol 2000; 220:424-31. [PMID: 10753528].

35. Thut CJ, Rountree RB, Hwa M, Kingsley DM. A large-scale in situ screen provides molecular evidence for the induction of eye anterior segment structures by the developing lens. Dev Biol 2001; 231:63-76. [PMID: 11180952].

36. Cvekl A, Tamm ER. Anterior eye development and ocular mesenchyme: new insights from mouse models and human diseases. BioEssays 2004; 26:374-86. [PMID: 15057935].

37. Gould DB, John SW. Anterior segment dysgenesis and the developmental glaucomas are complex traits. Hum Mol Genet 2002; 11:1185-93. [PMID: 12015278].

38. Zhang H, Deo M, Thompson RC, Uhler MD, Turner DL. Negative regulation of Yap during neuronal differentiation. Dev Biol 2012; 361:103-15. [PMID: 22037235].

39. Meisfeld JB, Gestri G, Clark BS, Flinn MA, Poole RJ, Bader JR, Besharse JC, Wilson SW, Link BA. Yap and Taz regulate retinal pigment epithelial cell fate. Development 2015; 142:3021-32. [PMID: 26209646].

40. Liu Y, Xin Y, Ye F, Wang W, Lu Q, Kaplan HJ, Dean DC. Taz-Tead1 links cell-cell contact to Zeb1 expression, proliferation, and dedifferentiation in retinal pigment epithelial cells. Biochem Mol Biol 2010; 51:3372-8. [PMID: 20207963].

41. Molday RS, Kellner U, Weber BH. X-linked juvenile retinoschisis: clinical diagnosis, genetic analysis and molecular mechanisms. Prog Retin Eye Res 2012; 31:195-212. [PMID: 22245536].

42. Johnson BA, Aoyama N, Friedell NH, Ikeda S, Ikeda A. Genetic modification of the schisis phenotype in a mouse model of X-linked retinoschisis. Genetics 2008; 178:1785-94. [PMID: 18245825].

43. Chen D, Xu T, Tu M, Xu J, Zhou C, Cheng L, Yang R, Yang T, Zheng W, He X, Deng R, Ge X, Li J, Song Z, Zhao J, Gu F. Recapitulating X-linked juvenile retinoschisis in mouse model by knock-in patient-specific novel mutation. Front Mol Neurosci 2018; 10:435-[PMID: 29379415].

44. Lian I, Kim J, Okazawa H, Zhao J, Zhao B, Yu J, Chinnaiyan A, Israel MA, Goldstein LS, Abujarour R, Ding S, Guan KL. The role of YAP transcription coactivator in regulating stem cell self-renewal and differentiation. Genes Dev 2010; 24:1106-18. [PMID: 20516196].

45. Nowell CS, Odermatt PD, Azzolin L, Hohnel S, Wagner EF, Fantner GE, Lutolf MP, Barrandon Y, Piccolo S, Radtke F. Chronic inflammation imposes aberrant cell fate in regenerating epithelia through mechanotransduction. Nat Cell Biol 2016; 18:168-80. [PMID: 26689676].

Articles are provided courtesy of Emory University and the Zhongshan Ophthalmic Center, Sun Yat-sen University, P.R. China. The print version of this article was created on 17 February 2019. This reflects all typographical corrections and errata to the article through that date. Details of any changes may be found in the online version of the article.